Cell death-inducing DNA fragmentation factor A-like effector A and fat-specific protein 27β coordinately control lipid droplet size in brown adipocytes

Received for publication, November 23, 2016, and in revised form, May 9, 2017 Published, Papers in Press, May 10, 2017, DOI 10.1074/jbc.M116.768820

Yuki Nishimoto[‡], Shinsuke Nakajima[‡], Sanshiro Tateya[‡§], Masayuki Saito[¶], Wataru Ogawa[‡], and Yoshikazu Tamori[‡‖1]

From the [‡]Department of Internal Medicine, Division of Diabetes and Endocrinology, Kobe University Graduate School of Medicine, Kobe 650-0017, Japan, [§]Department of Internal Medicine, Division of Diabetes, Kakogawa Central City Hospital, Kakogawa 675-8611, Japan, [¶]Department of Biomedical Sciences, Graduate School of Veterinary Medicine, Hokkaido University, Sapporo 060-0818, Japan, and [‖]Department of Internal Medicine, Division of Diabetes and Endocrinology, Chibune General Hospital, Osaka 555-0001, Japan

Edited by George M. Carman

Adipose tissue stores neutral lipids and is a major metabolic organ involved in regulating whole-body energy homeostasis. Triacylglycerol is stored as unilocular large lipid droplets (LDs) in white adipocytes and as multilocular small LDs in brown adipocytes. Proteins of the cell death-inducing DNA fragmentation factor A-like effector (Cide) family include CideA, CideB, and fat-specific protein of 27 (FSP27). Of these, FSP27 has been shown to play a crucial role in the formation of unilocular large LDs in white adipocytes. However, the mechanisms by which brown adipocytes store small and multilocular LDs remain unclear. An FSP27 isoform, FSP27β, was recently identified. We herein report that CideA and FSP27β are mainly expressed in brown adipose tissue and that FSP27β overexpression inhibits CideA-induced LD enlargements in a dose-dependent manner in COS cells. Furthermore, RNAi-mediated FSP27β depletion resulted in enlarged LDs in HB2 adipocytes, which possess the characteristics of brown adipocytes. Brown adipocytes in FSP27-knock-out mice that express CideA, but not FSP27β, had larger and fewer LDs. Moreover, we confirmed that FSP27β and CideA form a complex in brown adipose tissue. Our results suggest that FSP27β negatively regulates CideA-promoted enlargement of LD size in brown adipocytes. FSP27β appears to be responsible for the formation of small and multilocular LDs in brown adipose tissue, a morphology facilitating free fatty acid transport to mitochondria adjacent to LDs for oxidation in brown adipocytes.

Adipose tissue is specialized for storing neutral lipids and is one of the main metabolic organs involved in the regulation of whole-body energy homeostasis. There are two types of adipocytes (1): white adipocytes, which are energy-storing adipocytes, and brown adipocytes, which are energy-dissipating adipocytes. The former stores triacylglycerol (TAG)[2] effectively as unilocular large lipid droplets (LD) and supplies free fatty acids (FFAs) and glycerol to other tissues during fasting by hydrolyzing stored TAG. The latter consumes TAG stored as multilocular LD in order to generate heat through the mitochondrial oxidative phosphorylation of FFA and subsequent uncoupling in response to cold. The different morphologies of LD between these two types of adipose cells may reflect their unique characteristics.

Recent studies clarified that cell death-inducing DNA fragmentation factor A-like effector (Cide)-family proteins play a crucial role in lipid and energy metabolism including lipolysis, lipid oxidation, and LD formation (2). CideA is strongly expressed in brown adipocytes in mice (3), whereas CideB is mainly expressed in the liver and kidney (4). Fat-specific protein of 27 (FSP27) (CideC in humans) is abundantly expressed in adipose tissue and contributes to the formation of unilocular LD in white adipocytes (5–7). Although CideA and FSP27 are both involved in the formation of large LD (5–12), the molecular mechanisms by which brown adipocytes form multilocular small LD despite the abundant expression of CideA currently remain unknown. A new isoform of FSP27, FSP27β, was recently identified and is a molecule to which 10 amino acids were added to the amino-terminal domain of the conventional type of FSP27, designated as FSP27α (13). The expression of FSP27β in the liver is regulated by the liver-enriched transcription factor cyclic-AMP-responsive-element-binding protein H (CREBH) (13).

In the present study we investigated the mechanisms by which Cide-family proteins regulate the size and structure of LD in adipocytes and revealed that CideA and FSP27β regulate the formation of small and multilocular LD in brown adipocytes in a coordinated manner.

Results

Expression of FSP27α, FSP27β, and CideA in white and brown adipose tissues

We initially investigated the mRNA expression of FSP27α, FSP27β, and CideA in the epididymal white adipose tissue

This work was supported by the Japan Society for the Promotion of Science KAKENHI Grant 16K09748 (to Y. T.) The authors declare that they have no conflicts of interest with the contents of this manuscript.

[1] To whom correspondence should be addressed. Tel.: 81-78-382-5861; Fax: 81-78-382-2080; E-mail: tamori@med.kobe-u.ac.jp.

[2] The abbreviations used are: TAG, triacylglycerol; LD, lipid droplet(s); Cide, cell death-inducing DFF45-like effector; FSP27, fat-specific protein of 27; CREBH, cyclic-AMP-responsive element-binding protein H; BAT, brown adipose tissue; FFA, free fatty acid; (e)WAT, (epididymal) white adipose tissue; homo, homozygous; hetero, heterozygous.

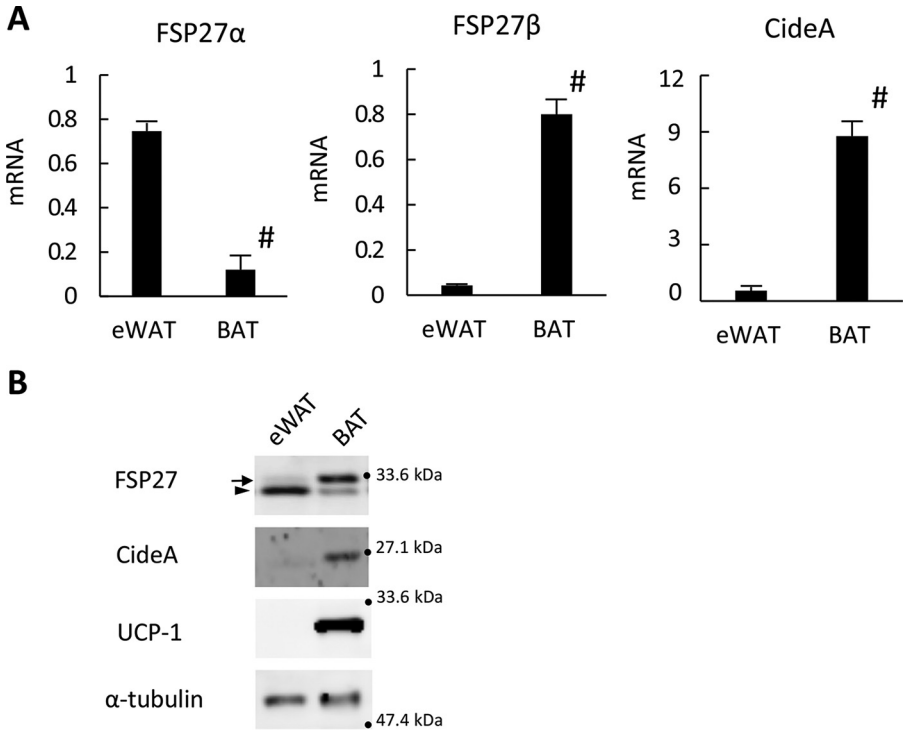

Figure 1. Expression of FSP27α, FSP27β, and CideA in white and brown adipose tissues. *A*, RT-PCR analysis of FSP27α, FSP27β, and CideA in the eWAT and BAT of C57BL/6J mice at 10 weeks of age. $n = 3$. # shows $p < 0.01$ *versus* eWAT. *B*, immunoblot analysis of FSP27α, FSP27β, and CideA in total cell lysates of the eWAT and BAT of C57BL/6J mice at 14 weeks of age. UCP-1 (BAT marker) and α-tubulin (loading control) were also examined. The *arrow* and *arrowhead* indicate FSP27β and FSP27α, respectively.

(eWAT) and brown adipose tissue (BAT) of mice using a quantitative RT-PCR method with primers that specifically recognize each isoform. FSP27α was mainly expressed in eWAT. In contrast, FSP27β and CideA were strongly expressed in BAT (Fig. 1*A*). We then confirmed the protein expression of these family members using an immunoblot analysis with an anti-CideA antibody and anti-FSP27 antibody that recognized the FSP27α and FSP27β isoforms. FSP27α was mainly expressed in eWAT, whereas FSP27β, which is 10 amino acids longer than FSP27α, was dominantly expressed in BAT (Fig. 1*B*). The CideA protein was specifically expressed in BAT (Fig. 1*B*). These results were consistent with those obtained on mRNA expression and suggest that FSP27α is expressed in eWAT, whereas FSP27β and CideA are expressed in BAT.

Effects of the overexpression of FSP27α, FSP27β, and CideA on the formation of LD in COS cells

We examined the effects of FSP27α, FSP27β, and CideA on the formation of LD in COS cells by overexpressing these proteins using a pIRES2-DSRed2 vector. We confirmed each protein expression in COS cells by immunoblot analysis. The expression level of FSP27α seems to be more abundant than FSP27β (Fig. 2*A*). The different expression levels between FSP27α and FSP27β may reflect the altered affinity of anti-FSP27 antibody to FSP27α and FSP27β due to the conformational difference between these two isoforms. In microscopic analysis, COS cells expressing these proteins were identified by monitoring the simultaneously expressed fluorescence marker DSRed. The overexpression of FSP27α resulted in the formation of large LD, as was reported previously (Fig. 2, *B* and *C*). At the same time, intracellular LD number was decreased significantly (Fig. 2, *B* and *D*). The overexpression of CideA also led to the formation of large LD and the decrease of intracellular LD number. However, LD sizes were smaller, and LD numbers were increased in cells overexpressing FSP27β than in control cells (Fig. 2, *B–D*). In the overexpression of FSP27β, the fluorescence marker protein DSRed2 was localized on the surface of LD (Fig. 2*B*); however, the reason for this localization of DSRed2 currently remains unknown. We then overexpressed FSP27α, FSP27β, and CideA in COS cells using a pcDNA3.1 vector and examined the intracellular localization of these molecules by immunofluorescence microscopy using an anti-FSP27 antibody and anti-CideA antibody. FSP27α and CideA both localized on the surface of large LD (Fig. 2*E*). FSP27β also localized around small LD (Fig. 2*E*). These results suggest that these three proteins are involved in LD formation on the LD surface.

A previous study reported that overexpression of COOH-terminal GFP-tagged FSP27β increased total cellular TAG content and LD size in COS cells (13). Therefore, to investigate the effects of FSP27β as a fusion protein in the LD formation, we overexpressed FSP27α, FSP27β, and CideA in COS cells as a fusion protein with the fluorescence protein DSRed-Monomer using the pDSRed-Monomer-C1 vector and examined the LD sizes and numbers. Immunofluorescence microscopy revealed that overexpression of FSP27α and CideA as a fusion protein with DSRed actually resulted in the large LD formation, although the degree of enlargement was slightly smaller than in the single expression (Fig. 3, *A* and *B*). Overexpression of

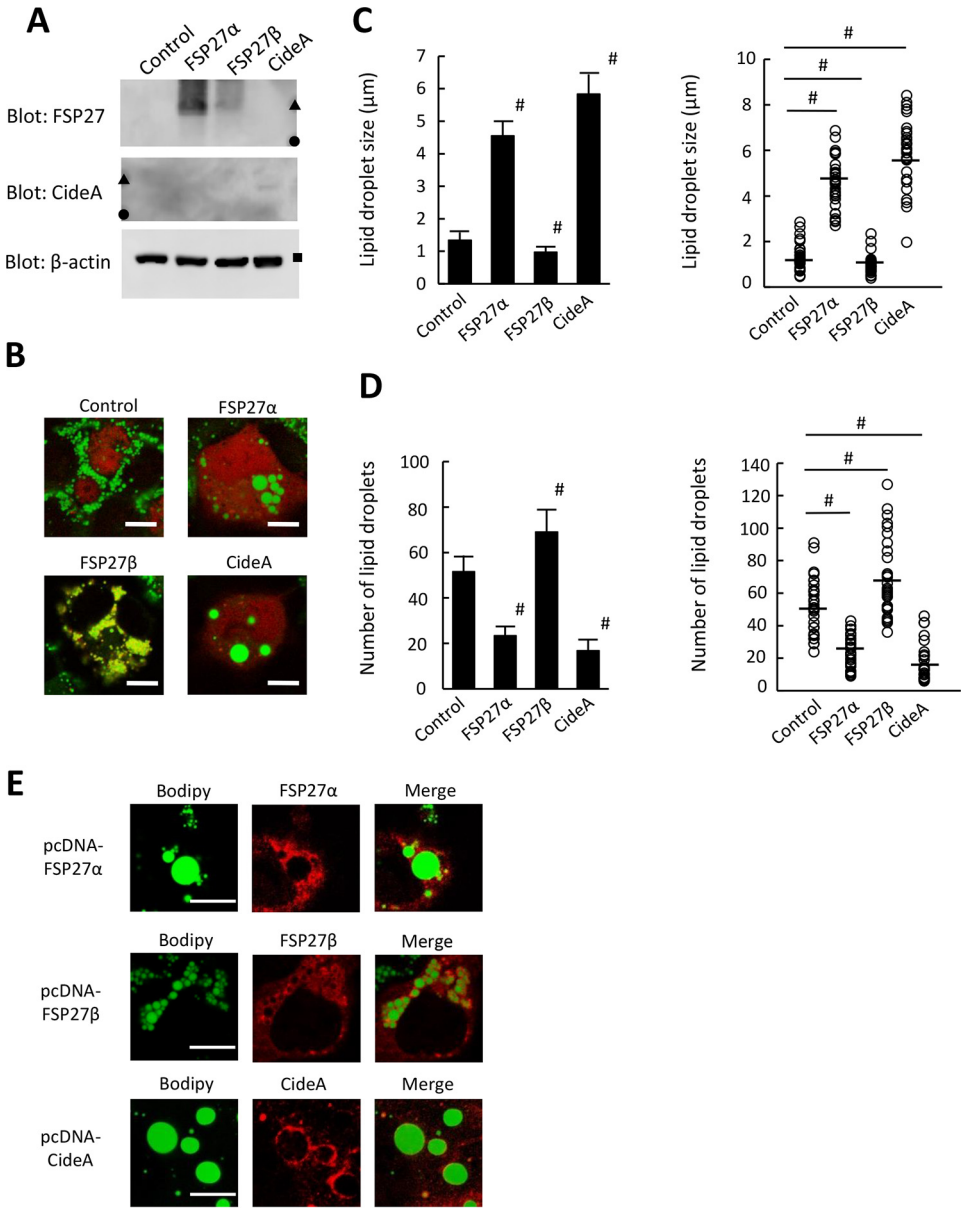

Figure 2. Effects of the overexpression of FSP27α, FSP27β, and CideA on LD sizes in COS cells. *A*, COS cells transfected with pIRES2-DSRed2 encoding FSP27α, FSP27β, or CideA were incubated with 400 μM oleic acid for 2 days and then subjected to immunoblot analysis with antibody against FSP27 and CideA. The *black triangle*, *circle*, and *square* represent molecular mass markers of 33.6 kDa, 27.1 kDa, and 47.5 kDa, respectively. β-Actin (loading control) was also examined. *B*, COS cells transfected with pIRES2-DSRed2 encoding FSP27α, FSP27β, or CideA along with the fluorescence marker DSRed2 were incubated with 400 μM oleic acid for 2 days and then stained with BODIPY 493/503 for triacylglycerol. A merged image of BODIPY 493/503 and DSRed2 fluorescence is shown. *Scale bar*: 10 μm. *C*, quantitation of LD sizes in COS cells expressing FSP27α, FSP27β, and CideA. Data are the means $\pm$ S.E. of the diameters of the largest LD in 30 cells (*left graph*). # shows $p < 0.01$ *versus* the control. The *right graph* is a scatter plot of the same results that shows all the data points and means. *D*, quantitation of intracellular LD numbers in COS cells expressing FSP27α, FSP27β, and CideA. Data are the means $\pm$ S.E. of the LD number in 30 cells. # shows $p < 0.01$ *versus* the control (*left graph*). The *right graph* is a scatter plot of the same results that shows all the data points and means. *E*, immunofluorescence localization of FSP27α, FSP27β, and CideA in COS cells by confocal laser microscopy. TAG was stained with BODIPY 493/503. The expression of FSP27α and FSP27β was detected with an anti-FSP27 antibody, whereas that of CideA was detected by an anti-CideA antibody. *Scale bar*: 10 μm.

FSP27β as a fusion protein with DSRed also increased the LD size very slightly compared with control even though the LD size was much smaller than FSP27α and CideA (Fig. 3, *A* and *B*). This is inconsistent with the result that overexpression of FSP27β solely decreased the LD size (Fig. 2, *B* and *C*). We assume this is because DSRed protein attached at the amino-terminal region could modify the original function of FSP27β. LD numbers were also decreased in cells overexpressing FSP27α and CideA as a fusion protein with DSRed (Fig. 3*C*). Three proteins were actually localized on the LD surface (Fig. 3*A*). These data clearly indicate that FSP27α and CideA, but not FSP27β, promote large LD formation and decreased intracellular LD number.

FSP27β inhibits the CideA-induced enlargement of LD in COS cells

Our results suggest that the main isoforms of the Cide family expressed in BAT are FSP27β and CideA. Thus, to reconstitute the condition of BAT, we overexpressed FSP27β and CideA in COS cells using the pIRES2-DSRed2 and pcDNA3.1 vectors,

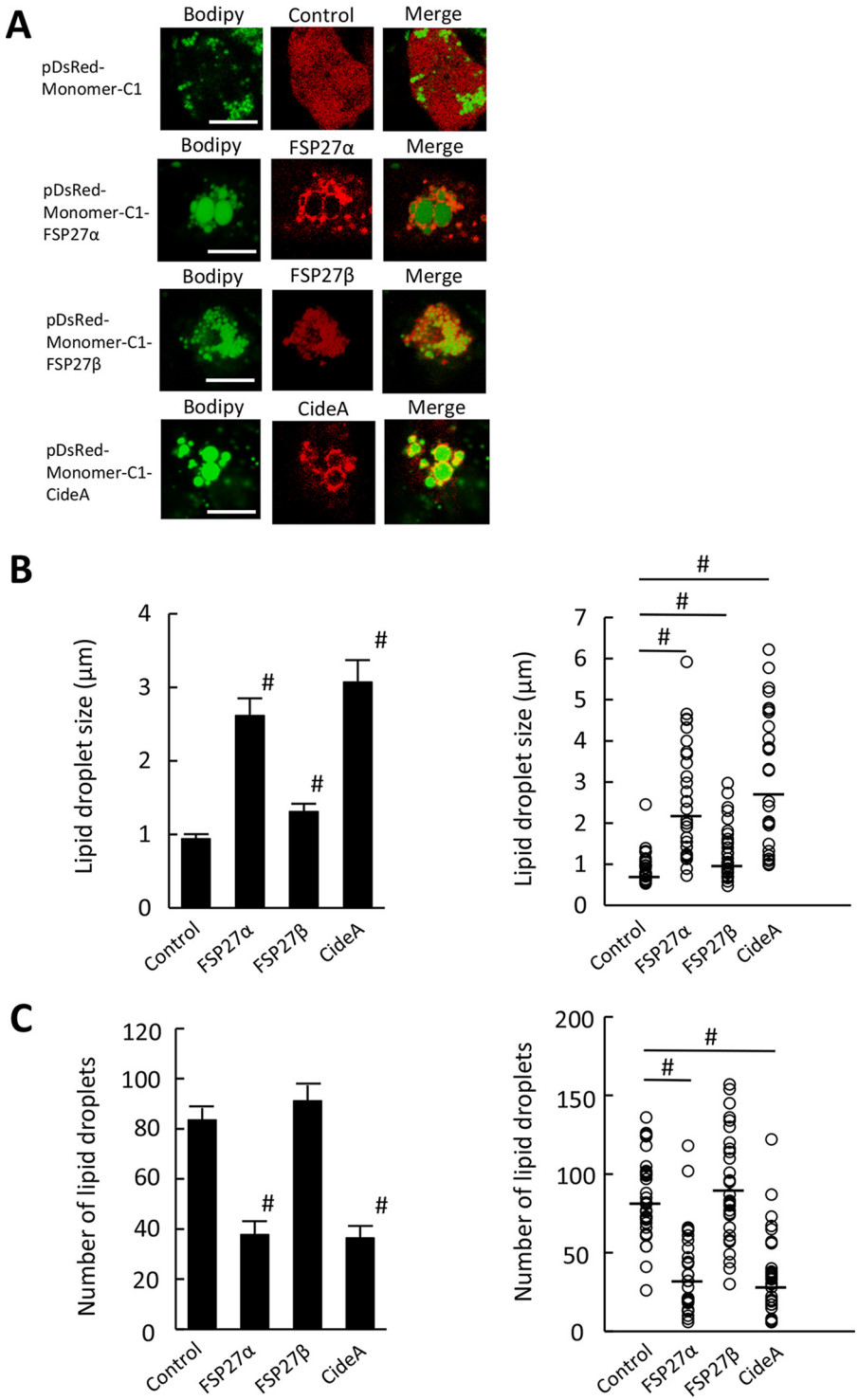

Figure 3. Effects of the overexpression of DSRed-Monomer-FSP27α, FSP27β, and CideA fusion proteins in COS cells. *A*, COS cells transfected with pDSRed-Monomer-C1 vectors encoding FSP27α, FSP27β, or CideA were incubated with 400 μM oleic acid for 2 days and then stained with BODIPY 493/503 for triacylglycerol. A merged image of BODIPY 493/503 and DSRed-Monomer fluorescence is shown. *Scale bar*: 10 μm. *B*, quantitation of LD sizes in COS cells expressing FSP27α, FSP27β, and CideA. Data are the means $\pm$ S.E. of the diameters of the largest LD in 30 cells. # shows $p < 0.01$ *versus* the control (*left graph*). The *right graph* is a scatter plot of the same results that shows all the data points and means. *C*, quantitation of intracellular LD numbers in COS cells expressing FSP27α, FSP27β, and CideA. Data are the means $\pm$ S.E. of the LD number in 30 cells. # shows $p < 0.01$ (*left graph*). The *right graph* is a scatter plot of the same results that shows all the data points and means.

respectively. We recognized cells overexpressing FSP27β by the fluorescence marker DSRed and those overexpressing CideA by immunofluorescence using an anti-CideA antibody. As shown in Fig. 4, *A* and *B*, the overexpression of CideA solely resulted in the formation of large LD. The overexpression of FSP27β did not induce large LD (Fig. 4, *A* and *B*). Furthermore, the simultaneous overexpression of FSP27β and CideA inhibited the CideA-induced large LD formation (Fig. 4, *A* and *B*).

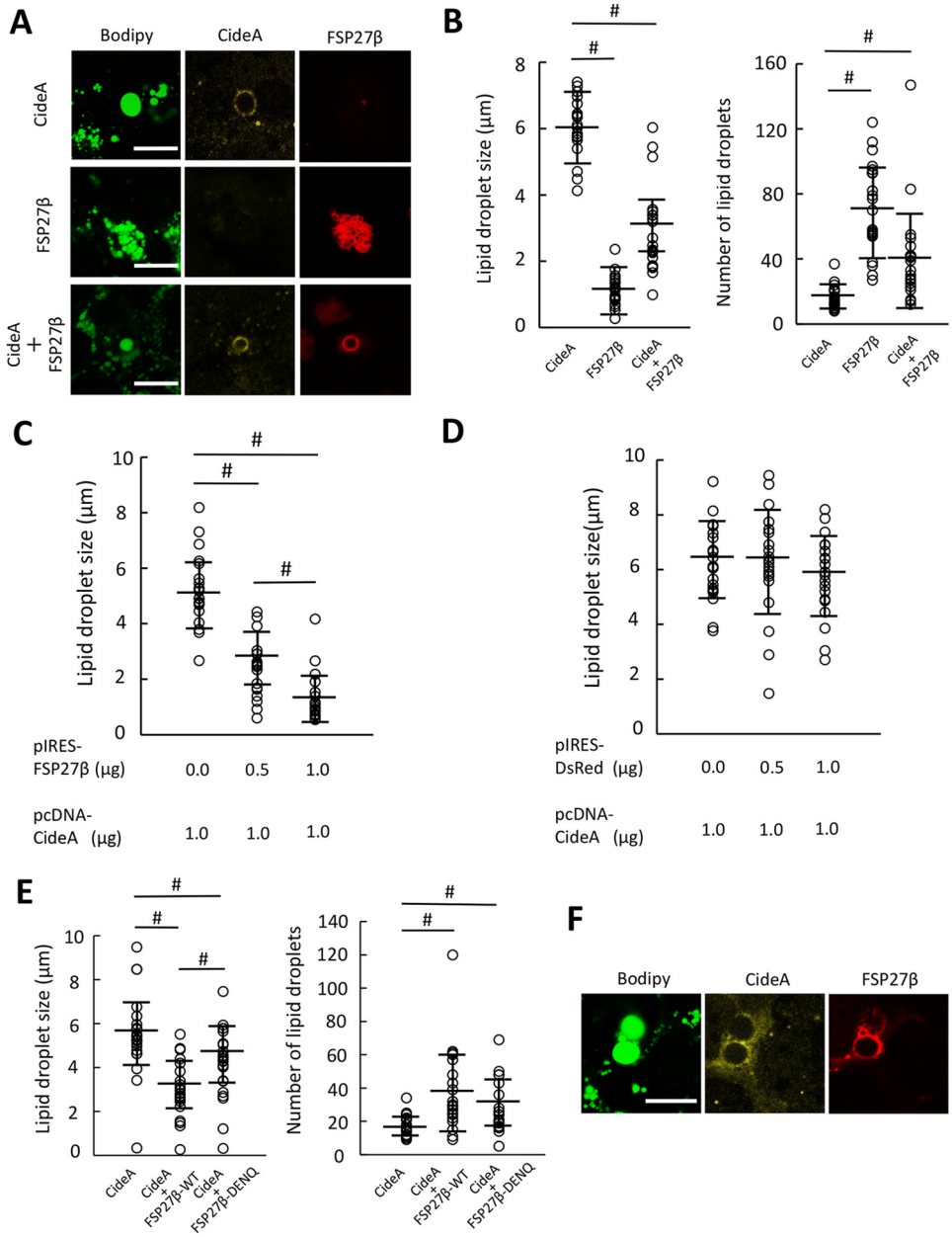

Figure 4. Effects of the overexpression of FSP27β on the CideA-induced enlargement of LD in COS cells. *A*, COS cells co-transfected with pcDNA encoding CideA and pIRES2-DsRed2 encoding DSRed2 and FSP27β were incubated with 400 μM oleic acid for 2 days and then stained with BODIPY 493/503 for triacylglycerol (*green*) followed by immunostaining for CideA using an anti-CideA primary antibody and anti-rabbit secondary antibody with Dylight405 and represented in *yellow*. *Scale bar*: 10 μm. *B*, quantitation of LD sizes (*left graph*) and numbers (*right graph*) in COS cells expressing FSP27β and CideA. Graphs represent all the data points with means ± S.D. $n = 20$. # shows $p < 0.01$ *versus* CideA. *C*, dose-dependent inhibition of CideA-induced enlargements in LD by FSP27β. Transfection was performed as in *A* in addition to changing the amount of the plasmids of pIRES2-DsRed2 encoding FSP27β. $n = 20$. # shows $p < 0.01$. *D*, quantitation of LD sizes in COS cells transfected as in *A* in addition to changing the amount of the plasmids of pIRES2-DSRed2. $n = 20$. *E*, quantitation of LD sizes (*left graph*) and numbers (*right graph*) in COS cells expressing CideA, FSP27β, and its mutant (*FSP27β-DENQ*). Graphs represent all the data points with means ± S.D. $n = 20$. # shows $p < 0.01$. *F*, immunofluorescence localization of CideA and FSP27β expressed by the pcDNA and pDSRed-Monomer-C1 vectors, respectively, in COS cells under confocal laser microscopy. TAG was stained with BODIPY 493/503 (*green*). The expression of FSP27β was detected with DSRed fluorescence, whereas that of CideA was detected by an anti-CideA antibody (*yellow*). *Scale bar*: 10 μm.

Co-overexpression of FSP27β and CideA increased intracellular LD numbers compared with CideA alone (Fig. 4, *A* and *B*). These results suggest that FSP27β dominantly inhibits the CideA-induced enlargement of LD and increases LD number. In addition, this inhibition of LD enlargement by the expression of FSP27β using the pIRES2-DSRed2 vector was dose-dependent (Fig. 4*C*), although the control pIRES2-DSRed2 vectors showed no effect on LD size (Fig. 4*D*). In the previous study, we produced the mutant of FSP27α in which the negatively charged acidic polar amino acids (Asp-215, Glu-218, Glu-219, and Glu-220), which are supposed to be important for dimer formation, were replaced by noncharged polar amino acids (Asn-215, Gln-218, Gln-219, and Gln-220) and revealed that these negatively charged acidic polar amino acids (Asp-215, Glu-218, Glu-219, and Glu-220) were indispensable for the function of FSP27α to enlarge LD (12). Therefore, we introduced the same mutations to FSP27β to decrease the function of FSP27β and examined the inhibitory effect of FSP27β to

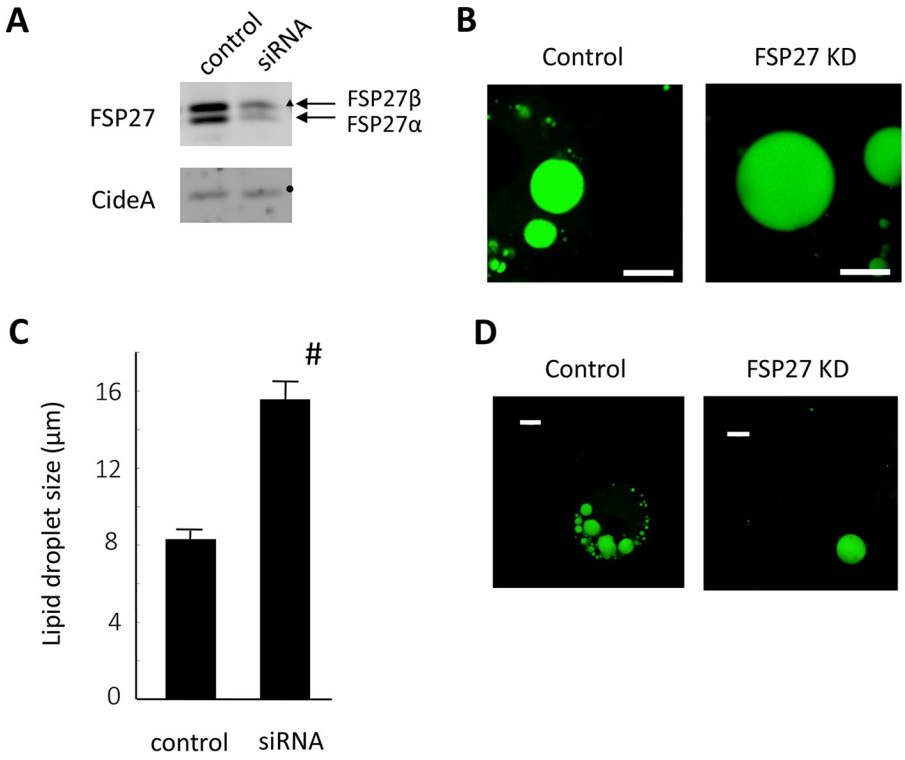

Figure 5. Effects of FSP27β depletion by siRNA on LD sizes in HB2 adipocytes. *A*, immunoblot analysis of FSP27α, FSP27β, and CideA in HB2 adipocytes in which FSP27α and FSP27β were depleted using siRNA. The *black triangle* and *circle* represent molecular mass markers of 33.6 kDa and 27.1 kDa, respectively. *B*, HB2 adipocytes were stained with BODIPY 493/503 for triacylglycerol for 2 days after the knockdown with siRNA. *Scale bar*: 10 μm. *C*, quantitation of LD sizes in HB2 adipocytes in which FSP27α and FSP27β were depleted with siRNA. Data are the means $\pm$ S.E. of the diameters of the largest LD in 35 cells. # shows $p <$ 0.01 *versus* control cells. *D*, typical LD pattern in HB2 adipocytes stained with BODIPY 493/503 for triacylglycerol for 2 days after the knockdown with siRNA. *Scale bar*: 10 μm.

CideA-induced LD enlargement. We found that the effect of the mutant FSP27β to inhibit the enlargement of LD size promoted by CideA was diminished compared with wild-type FSP27β (Fig. 4*E*), suggesting that FSP27β is actually involved in the regulation of LD size. Next, to investigate the intracellular localization of FSP27β and CideA in cells expressing both proteins in more detail, we overexpressed FSP27β and CideA in COS cells using the pDSRed-Monomer-C1 and pcDNA3.1 vectors, respectively. Immunofluorescence microscopy revealed that the red fluorescence of DSRed fused with FSP27β showed the same distribution to the fluorescence of CideA recognized by immunofluorescence using the anti-CideA antibody (Fig. 4*F*). These results suggest that FSP27β inhibits the function of CideA that enlarges LD at the same region on the LD surface.

Depletion of FSP27β resulted in the enlargement of LD in brown adipocytes

To confirm that FSP27β plays an inhibitory role in CideA-induced LD enlargements in brown adipocytes, we depleted the expression of FSP27β in the brown adipocyte cell line, HB2, which was established from the preadipocytes of mouse BAT (14). After the induction of adipogenesis, HB2 cells showed the morphological characteristics of brown adipocytes, including the formation of multilocular small LD in the cytoplasm. These cultured brown adipocytes also expressed FSP27β, CideA, and FSP27α (Fig. 5*A*). In these cells almost similar amounts of proteins in FSP27α and FSP27β were expressed. This is because HB2 cells are the established cultured adipocytes, and their characters as brown fat cells are thought to get weaker compared with their original brown fat cells in which FSP27β is overwhelmingly expressed. The results of the immunoblot analysis revealed that the knockdown of FSP27 using siRNA markedly decreased endogenous FSP27α and -β without affecting the expression of CideA (Fig. 5*A*). The decreased expression of FSP27α and -β enlarged LD in HB2 brown adipocytes (Fig. 5, *B* and *C*). In addition, many cells presented unilocular LD in knockdown of FSP27, although almost all control cells displayed multilocular LD pattern (Fig. 5*D*). Given that the function of FSP27α is the formation of large and unilocular LD, the result obtained by the knockdown of FSP27 was due to the decrease of FSP27β. We also examined the size of LD in the BAT of FSP27 knock-out (KO) mice. FSP27 was not expressed in eWAT and BAT in FSP27 homo KO mice, although CideA expression levels in BAT did not change among wild-type, FSP27 hetero KO, and FSP27 homo KO mice (Fig. 6*A*). As demonstrated previously, the size of LD markedly decreased in the eWAT of FSP27 homo KO mice (Fig. 6, *B* and *C*). In contrast, the size of LD was markedly larger in the BAT of FSP27 homo KO mice than in that of wild-type or hetero KO mice (Fig. 6, *B* and *C*). The number of LD in the BAT of FSP27 homo KO mice decreased, and the formation of LD shifted more toward unilocular LD (Fig. 6, *B* and *D*). These results suggest that FSP27β plays an inhibitory role in the CideA-induced enlargement of LD in brown adipocytes.

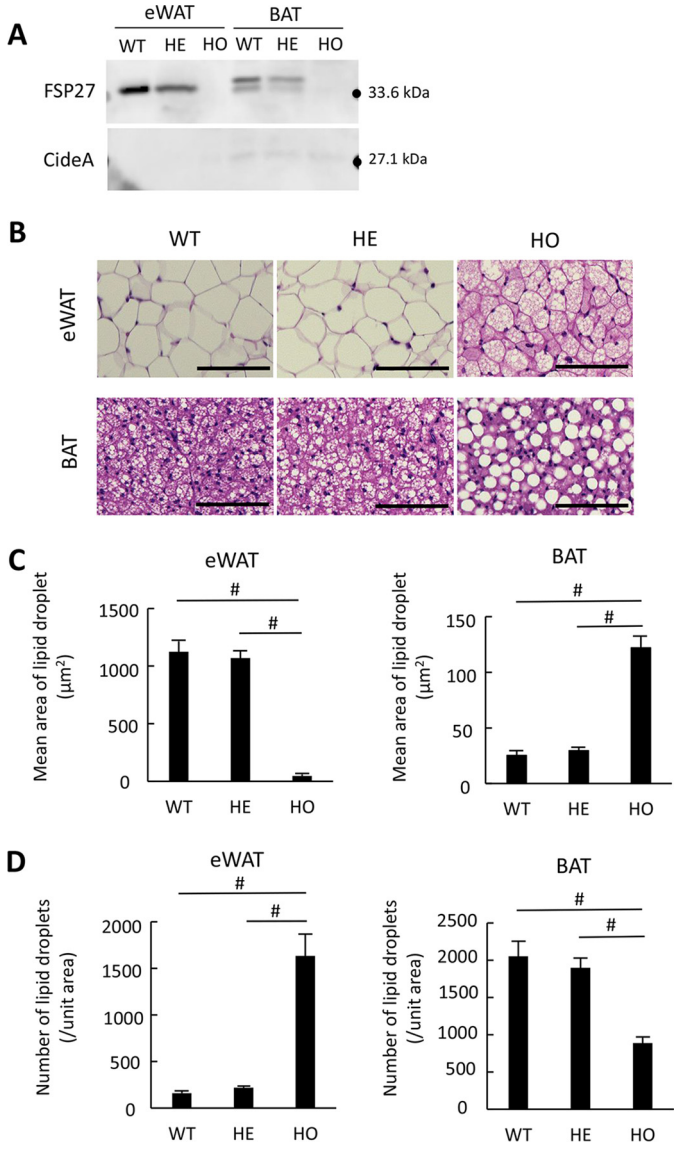

Figure 6. LD size and number in white and brown adipocytes from FSP27 knock-out mice. *A*, immunoblot analysis of FSP27 and CideA protein in eWAT and BAT from wild-type (*WT*), FSP27 hetero KO (*HE*), and FSP27 homo KO (*HO*) mice. *B*, sections of eWAT and BAT from WT, FSP27 hetero KO (*HE*), and FSP27 homo KO (*HO*) mice were stained by hematoxylin-eosin and examined by light microscopy. *Scale bar*: 100 μm. *C*, quantitation of LD sizes in eWAT and BAT from wild-type (*WT*), FSP27 hetero KO (*HE*), and FSP27 homo KO (*HO*) mice. $n = 1{,}593$ (*WT*), 2,201 (*HE*), and 16,355 (*HO*) in eWAT and 20,372 (*WT*), 18,953 (*HE*), and 8,243 (*HO*) in BAT. # shows $p < 0.01$. *D*, comparison of LD numbers in a unit area of eWAT and BAT from wild-type (*WT*), FSP27 hetero KO (*HE*), and FSP27 homo KO (*HO*) mice. # shows $p < 0.01$. The LD area in *C* and LD number in *D* were measured with BZ-X710, Keyence.

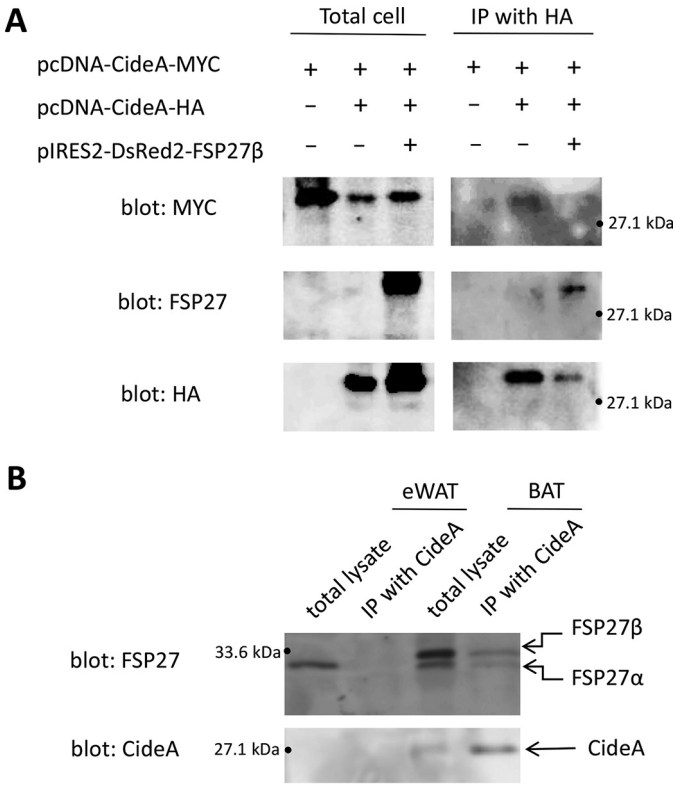

Figure 7. FSP27β inhibits the homo dimerization of CideA in COS cells and forms a complex with CideA in BAT. *A*, overexpression of FSP27β inhibits the homodimer formation of CideA in COS cells. Extracts of COS cells transfected with an expression vector pcDNA encoding CideA-MYC alone, CideA-MYC, and CideA-HA with or without a vector pIRES2-DSRed2 encoding FSP27β, as indicated, were subjected to immunoprecipitation (*IP*) with antibody to HA. Total cells and immunoprecipitates were subsequently subjected to immunoblot analysis with antibody to MYC, FSP27, and HA. Total amounts of plasmids in each cell were adjusted to the same by adding pcDNA and pIRES2-DSRed2 vectors. *B*, detergent extracts of the BAT and eWAT of 9-week old mice were subjected to immunoprecipitation with the antibody against CideA. Total cell lysates and the resulting immunoprecipitates were analyzed with an immunoblot analysis using antibodies to FSP27 and CideA.

FSP27β inhibits the homo dimerization of CideA in COS cells and actually forms a complex with CideA in brown adipocytes

Previous studies proposed that not only FSP27α, but also CideA, promote LD growth by forming a homodimer on the contact site of two contiguous LD and inducing their fusion (15–17). Because FSP27β inhibited the CideA-induced enlargement of LD, FSP27β may bind to CideA, resulting in the inhibition of the homodimer of CideA and subsequent growth of LD in brown adipocytes. Thus, we investigated whether FSP27β inhibited the homodimer formation of CideA in COS cells. We overexpressed CideA tagged with human c-MYC (CideA-MYC) or tagged with human influenza hemagglutinin (HA) (CideA-HA) using the pcDNA3.1 vector. CideA-MYC was co-immunoprecipitated with CideA-HA using the antibody to HA from the detergent extracts of COS cells expressing both CideA-MYC and CideA-HA, suggesting that CideA actually forms a homodimer (Fig. 7*A*). Additional overexpression of FSP27β in cells expressing both CideA-MYC and CideA-HA resulted in the co-immunoprecipitation of FSP27β and the simultaneous decrease of co-immunoprecipitated CideA-MYC with CideA-HA using antibody to HA, indicating that FSP27β inhibited the homodimer formation of CideA by binding to CideA. Finally, we investigated whether CideA and FSP27β indeed formed a complex in brown adipocytes. We confirmed that FSP27β co-immunoprecipitated with CideA using an anti-CideA antibody from detergent extracts of the BAT of wild-type mice (Fig. 7*B*), which indicates that FSP27β binds to CideA in brown adipocytes. However, we failed to confirm the complex formation between CideA and FSP27β by the immunoprecipitation experiment using anti-FSP27 antibody (data not shown). We speculate this is because our antibody to FSP27 can not identify FSP27 that forms a complex with CideA.

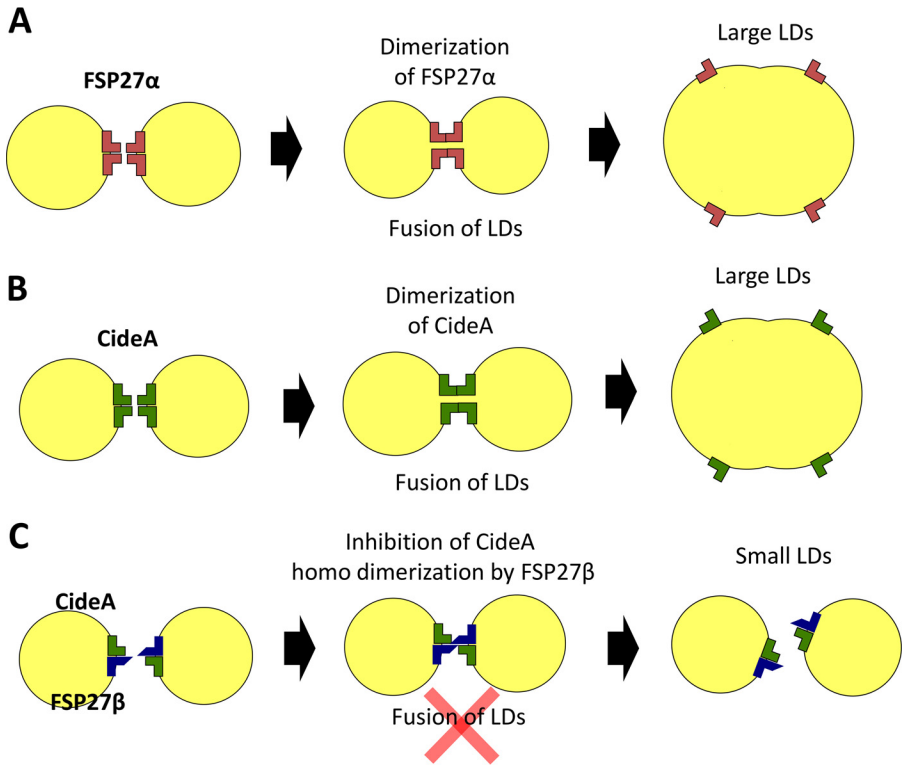

Figure 8. Proposed mechanisms by which the Cide protein family regulates LD sizes in WAT and BAT. In WAT, FSP27α on neighboring LD induces homo dimerization, resulting in the fusion of LD, subsequent lipid exchange, and formation of larger LD (*A*). CideA also mediates the formation of large LD in the same manner (*B*). In BAT, FSP27β inhibits the homo dimerization of CideA and suppresses the formation of large LD (*C*).

Discussion

In the present study we confirmed that FSP27β, a recently identified isoform of FSP27 abundantly expressed in BAT, plays a critical role in the formation of small LD in brown adipocytes by working co-operatively with CideA. FSP27α and CideA are enriched at a particular sub-LD location: the LD-LD contact site (15, 16). They are both assumed to form a homodimer between contacting LD and mediate LD fusion and growth. Because CideA and FSP27β are both localized on the LD surface and form a complex, FSP27β is assumed to decrease enlargements in LD by inhibiting the homodimerization of CideA (Fig. 8). This result provides an insight into the mechanisms underlying the formation of small and multilocular LD in BAT.

Adipocytes are required not only to store TAG but also to rapidly hydrolyze TAG in WAT for the supply of FFA to other tissues through the circulation during fasting or for heat production in mitochondria in BAT. Therefore, the unilocular LD form is ideal in WAT because of the efficient storage of TAG and efflux of hydrolyzed FFA from the cell surface to the circulation. FSP27α has been suggested to promote the growth of LD by mediating the fusion of contacting LD through the dimerization of FSP27 proteins focally enriched at the contact site between LD (15, 18). In addition, FSP27α is associated with several proteins including perilipin (18, 19) and adipocyte triacylglycerol lipase (20). Because isoproterenol-stimulated lipolysis was previously reported to be impaired in the isolated white adipocytes of FSP27 KO mice (5), FSP27α may also contribute to rapid and efficient lipolysis through these proteins in addition to TAG storage. In contrast, in BAT, the formation of multilocular small LD is important for the efficient influx of hydrolyzed FFA to the adjacent mitochondria for β oxidation and subsequent heat production. O_2 consumption stimulated by a β3-adrenergic agonist was found to be reduced in isolated brown adipocytes representing the formation of large LD in FSP27 KO mice (5). Furthermore, FSP27α may play important roles in rapid lipolysis through adipocyte triacylglycerol lipase (20); therefore, FSP27β may also be indispensable for rapid and efficient lipolysis in association with lipases in BAT.

In the present study we demonstrated that CideA and FSP27β were mainly expressed in BAT, and the overexpression of CideA promoted the formation of large LD to a similar degree as FSP27α in COS cells. A previous study detected multilocular LD in WAT along with the enlargement of LD in BAT from FSP27 KO mice in which FSP27α and FSP27β were both depleted (5). These phenotypes are explained by the present results showing that FSP27β inhibits enlargements in LD in brown adipocytes. In contrast, our results are inconsistent with previous findings demonstrating that the overexpression of FSP27β promotes the enlargement of LD in COS7 cells, although the LD size was not quantitated (13). The reason for this difference currently remains unknown. However, it may be related to FSP27β being expressed as a fusion protein with GFP in COS cells in the previous study (13). In fact, FSP27β expressed as a fusion protein with DSRed in COS cells increased LD size to a small degree in the present study, although the increased level of LD size was much smaller compared with CideA and FSP27α.

CREBH is a liver-enriched transcription factor localized in the endoplasmic reticulum (ER) membrane and is activated

by ER stress or inflammatory stimuli to induce acute-phase hepatic inflammation (21). This transcription factor has also been shown to regulate glucose and lipid metabolism (22–24). CREBH was recently reported to directly bind to the CREBH response element in the 5′-flanking region of the FSP27 gene and to play a critical role in the expression of FSP27β in the liver (13). Although FSP27β is a major isoform of FSP27 in BAT, CREBH was not expressed in BAT (13). Therefore, the mechanisms responsible for regulating the expression of FSP27β in BAT remain unclear. Further studies to elucidate the mechanisms by which the expression of FSP27β is regulated in BAT will be important for the development of new therapies to modulate energy metabolism. In conclusion, we herein demonstrated that FSP27β and CideA co-operatively form small multilocular LD, which is an advantageous morphology for the transport of FFA to mitochondria adjacent to LD for oxidation in brown adipocytes.

Experimental procedures

Plasmids

Full-length mouse FSP27α was obtained as described previously (5). The full-length complementary DNA (cDNA) of mouse CideA was obtained by reverse transcription and a polymerase chain reaction (RT-PCR) with the specific oligonucleotide primers (5′-ATGGAGACCGCCAGGGACTAC-3′ (sense) and 5′-CCGCGGTTACATGAACCAGCCTTTG-3′ (antisense)) and total RNA from mouse brown adipose tissue. The full-length cDNA of mouse FSP27β was obtained by PCR with the specific oligonucleotide primers (5′-ATGGAGTCCAACACAATCCAACTGACAAGGATGGACTACGCCATGAAG-3′ (sense) and 5′-AACCGCGGTCATTGCAGCATCTTCAGACAGG-3′ (antisense)) and cDNA of mouse FSP27α. The base sequences of each clone were confirmed by DNA sequencing. The full-length cDNAs of mouse FSP27α, FSP27β, and CideA were subcloned into the pcDNA3.1 (Invitrogen), pIRES2-DsRed2 (Clontech), or pDSRed-Monomer-C1 (Clontech) vector. CideA was tagged with human c-MYC or human HA epitopes by adding (at the cDNA level) a 10-amino acid sequence (EQKLISEEDL) and 9-amino acid sequence (YPYDVPDYA) at their COOH termini, respectively.

Quantitative RT-PCR

cDNA synthesized from total RNA extracted from mouse tissues using an RNeasy kit (QUIAGEN) was analyzed in a Sequence Detector (model 7500; PE Applied Biosystems) with specific primers and Power SYBR Green PCR Master Mix (Applied Biosystems). The relative abundance of mRNAs was calculated with 36B4 mRNA as the invariant control. The following primers (sense and antisense, respectively) were used: FSP27α, 5′-GCCACGCGGTATTGCCAGGA-3′ and 5′-GGGTCTCCCGGCTGGGCTTA-3′; FSP27β, 5′-GTGACCACAGCTTGGGTCGGA-3′ and 5′-GGGTCTCCCGGCTGGGCTTA-3′; CideA, 5′-ATGGAGACCGCCAGGGACTAC-3′ and 5′-GCTACTTCGGTCATGGTTTG-3′.

Cell culture and FSP27 knock-out mice

COS cells were cultured in Dulbecco's modified Eagle's medium (DMEM) (Sigma) containing 10% fetal bovine serum (FBS) (Biowest). HB2 cells were prepared from the interscapular BAT of p53 homozygous knock-out mice, as described previously (14). Cells were maintained in DMEM supplemented with 10% FBS (JRH Biosciences), streptomycin (50 μg/ml), and penicillin (50 units/ml). At confluence, fresh medium supplemented with 0.5 mM 3-isobutyl-1-methylxanthine and 1 nM dexamethasone was added to cells for the induction of adipocyte differentiation. After 2 days, medium was changed to DMEM supplemented with 50 nM triiodothyronine and insulin (10 μg/ml) and was refreshed every 2 days. FSP27 KO mice were generated as previously described (5). Experimental protocols with mice were approved by the Animal Ethics Committee of Kobe University Graduate School of Medicine.

Depletion of FSP27 in HB2 adipocytes

Five days after the onset of induction of differentiation, HB2 adipocytes were washed twice with PBS, detached from the culture dish by exposure to 0.25% trypsin and collagenase (0.5 mg/ml) in PBS, and resuspended in phosphate-buffered saline (PBS). The cells ($\sim 3 \times 10^6$) were then mixed with siRNA duplexes and subjected to electroporation with a Bio-Rad Gene Pulser II system at a setting of 0.18 kV and 0.975 microfarads. The FSP27 siRNA was targeted to the mRNA sequence 5′-GCACAAUCGUGGAGACAGAAGAAUA-3′. Immediately after electroporation, the cells were mixed with fresh DMEM supplemented with 10% FBS, and 10 min later they were seeded onto culture plates. They were subjected to assays 2 days after electroporation.

Overexpression of FSP27 and CideA proteins in COS cells and a microscopic analysis

Expression plasmids were introduced into COS cells using X-tremeGENE 9 DNA Transfection Reagent (Roche Applied Science). Before the microscopic analysis, cells were incubated with BODIPY 493/503 (Invitrogen) for the detection of LD at 37 °C for 5 min in a cell incubator. Cells were then fixed with PBS containing 4% paraformaldehyde at room temperature, washed with PBS, and exposed to PBS containing 5% bovine serum albumin (BSA). In the immunostaining of FSP27 and CideA, cells were permeabilized with 0.2% Triton X-100 for 5 min and incubated with PBS containing 5% BSA. They were then visualized by indirect immunofluorescence staining with an anti-FSP27 antibody and anti-CideA antibody followed with an Alexa-Fluor555-conjugated goat antibody to rabbit IgG (Invitrogen) or Dylight405-conjugated goat antibody to rabbit IgG (Thermo Scientific). Cells were then examined with a confocal laser-scanning microscope (LSM700, Carl Zeiss). LD sizes in each cell were obtained by measuring the diameter of the largest LD in cells using the measuring instrument installed in the confocal laser-scanning microscope.

Immunoblot and immunoprecipitation analysis

Cell lysates were prepared with lysis buffer containing 25 mM Tris-HCl (pH 7.4), 150 mM NaCl, 1 mM EDTA, 1% Triton X-100, 50 mM NaF, 10 mM sodium pyrophosphate, 1 mM sodium vanadate, and 1 mM phenylmethanesulfonyl fluoride. Adipose tissue homogenates were prepared in the same buffer or CelLytic MT Cell Lysis Reagent (Sigma) using a Teflon

homogenizer. In eWAT and BAT, tissue homogenates were subjected to the immunoprecipitation at 4 °C for 3 h with antibodies to CideA. Tissue extracts and the resulting immunoprecipitates were subjected to an immunoblot analysis with antibodies to FSP27 and CideA. In COS cells, detergent extracts were subjected to the immunoprecipitation at 4 °C for 3 h with antibodies to HA. Total cell and the resulting immunoprecipitates were subjected to an immunoblot analysis with antibodies to MYC, FSP27, and HA. The polyclonal antibody to FSP27 was generated by injecting rabbits with a glutathione *S*-transferase fusion protein of mouse FSP27 (amino acid residues 45–127) that was expressed in and purified from *Escherichia coli*. A rabbit antibody to CideA was purchased from Santa Cruz Biotechnology. Mouse antibodies to α-tubulin and β-actin were purchased from Sigma. A rabbit polyclonal antibody to UCP-1 was purchased from Abcam. Anti-HA antibody produced in rabbit and anti-MYC monoclonal antibody 9E10 was purchased from Sigma and Santa Cruz Biotechnology, respectively.

Histological analysis of mouse BAT

The WAT and BAT of mice were fixed with formalin, embedded in paraffin, sectioned at a thickness of 6 μm, and mounted on glass slides using standard procedures. Sections were stained with hematoxylin-eosin. The area and number of LD were measured by fluorescence microscopy (BZ-X710, Keyence).

Statistical analysis

Quantitative data are expressed as the mean ± S.E or ± S.D. The significance of differences between groups was examined with a two-tailed Student's *t* test. Differences were considered significant at $p < 0.05$.

Author contributions—Y. N. and S. N. performed the experiments. S. T. analyzed the data. M. S. contributed the reagents/materials/analysis tools. W. O. commented extensively on the data and manuscript. Y. T. conceived and designed the experiment and wrote the manuscript. All authors reviewed the results and approved the manuscript.

Acknowledgment—We thank S. Shigeta for technical assistance as well as H. Bando for technical advice.

References

1. Cohen, P., and Spiegelman, B. M. (2016) Cell biology of fat storage. *Mol. Biol. Cell* **27,** 2523–2527
2. Xu, L., Zhou, L., and Li, P. (2012) CIDE proteins and lipid metabolism. *Arterioscler. Thromb. Vasc. Biol.* **32,** 1094–1098
3. Zhou, Z., Yon Toh, S., Chen, Z., Guo, K., Ng, C. P., Ponniah, S., Lin, S. C., Hong, W., and Li, P. (2003) Cidea-deficient mice have lean phenotype and are resistant to obesity. *Nat. Genet.* **35,** 49–56
4. Li, J. Z., Ye, J., Xue, B., Qi, J., Zhang, J., Zhou, Z., Li, Q., Wen, Z., and Li, P. (2007) Cideb regulates diet-induced obesity, liver steatosis, and insulin sensitivity by controlling lipogenesis and fatty acid oxidation. *Diabetes* **56,** 2523–2532
5. Nishino, N., Tamori, Y., Tateya, S., Kawaguchi, T., Shibakusa, T., Mizunoya, W., Inoue, K., Kitazawa, R., Kitazawa, S., Matsuki, Y., Hiramatsu, R., Masubuchi, S., Omachi, A., Kimura, K., Saito, M., *et al.* (2008) FSP27 contributes to efficient energy storage in murine white adipocytes by promoting the formation of unilocular lipid droplets. *J. Clin. Invest.* **118,** 2808–2821
6. Puri, V., Konda, S., Ranjit, S., Aouadi, M., Chawla, A., Chouinard, M., Chakladar, A., and Czech, M. P. (2007) Fat-specific protein 27, a novel lipid droplet protein that enhances triglyceride storage. *J. Biol. Chem.* **282,** 34213–34218
7. Toh, S. Y., Gong, J., Du, G., Li, J. Z., Yang, S., Ye, J., Yao, H., Zhang, Y., Xue, B., Li, Q., Yang, H., Wen, Z., and Li, P. (2008) Up-regulation of mitochondrial activity and acquirement of brown adipose tissue-like property in the white adipose tissue of fsp27-deficient mice. *PLoS ONE* **3,** e2890
8. Puri, V., Ranjit, S., Konda, S., Nicoloro, S. M., Straubhaar, J., Chawla, A., Chouinard, M., Lin, C., Burkart, A., Corvera, S., Perugini, R. A., and Czech, M. P. (2008) Cidea is associated with lipid droplets and insulin sensitivity in humans. *Proc. Natl. Acad. Sci. U.S.A.* **105,** 7833–7838
9. Christianson, J. L., Boutet, E., Puri, V., Chawla, A., and Czech, M. P. (2010) Identification of the lipid droplet targeting domain of the Cidea protein. *J. Lipid Res.* **51,** 3455–3462
10. Keller, P., Petrie, J. T., De Rose, P., Gerin, I., Wright, W. S., Chiang, S. H., Nielsen, A. R., Fischer, C. P., Pedersen, B. K., and MacDougald, O. A. (2008) Fat-specific protein 27 regulates storage of triacylglycerol. *J. Biol. Chem.* **283,** 14355–14365
11. Jambunathan, S., Yin, J., Khan, W., Tamori, Y., and Puri, V. (2011) FSP27 promotes lipid droplet clustering and then fusion to regulate triglyceride accumulation. *PLoS ONE* **6,** e28614
12. Tamori, Y., Tateya, S., Ijuin, T., Nishimoto, Y., Nakajima, S., and Ogawa, W. (2016) Negatively charged residues in the polar carboxy-terminal region in FSP27 are indispensable for expanding lipid droplets. *FEBS Lett.* **590,** 750–759
13. Xu, X., Park, J. G., So, J. S., and Lee, A. H. (2015) Transcriptional activation of Fsp27 by the liver-enriched transcription factor CREBH promotes lipid droplet growth and hepatic steatosis. *Hepatology* **61,** 857–869
14. Irie, Y., Asano, A., Cañas, X., Nikami, H., Aizawa, S., and Saito, M. (1999) Immortal brown adipocytes from p53-knockout mice: differentiation and expression of uncoupling proteins. *Biochem. Biophys. Res. Commun.* **255,** 221–225
15. Gong, J., Sun, Z., Wu, L., Xu, W., Schieber, N., Xu, D., Shui, G., Yang, H., Parton, R. G., and Li, P. (2011) Fsp27 promotes lipid droplet growth by lipid exchange and transfer at lipid droplet contact sites. *J. Cell Biol.* **195,** 953–963
16. Barneda, D., Planas-Iglesias, J., Gaspar, M. L., Mohammadyani, D., Prasannan, S., Dormann, D., Han, G. S., Jesch, S. A., Carman, G. M., Kagan, V., Parker, M. G., Ktistakis, N. T., Klein-Seetharaman, J., Dixon, A. M., Henry, S. A., and Christian, M. (2015) The brown adipocyte protein CIDEA promotes lipid droplet fusion via a phosphatidic acid-binding amphipathic helix. *Elife* **4,** e07485
17. Lee, S. M., Jang, T. H., and Park, H. H. (2013) Molecular basis for homo-dimerization of the CIDE domain revealed by the crystal structure of the CIDE-N domain of FSP27. *Biochem. Biophys. Res. Commun.* **439,** 564–569
18. Sun, Z., Gong, J., Wu, H., Xu, W., Wu, L., Xu, D., Gao, J., Wu, J. W., Yang, H., Yang, M., and Li, P. (2013) Perilipin1 promotes unilocular lipid droplet formation through the activation of Fsp27 in adipocytes. *Nat. Commun.* **4,** 1594
19. Grahn, T. H., Zhang, Y., Lee, M. J., Sommer, A. G., Mostoslavsky, G., Fried, S. K., Greenberg, A. S., and Puri, V. (2013) FSP27 and PLIN1 interaction promotes the formation of large lipid droplets in human adipocytes. *Biochem. Biophys. Res. Commun.* **432,** 296–301
20. Grahn, T. H., Kaur, R., Yin, J., Schweiger, M., Sharma, V. M., Lee, M. J., Ido, Y., Smas, C. M., Zechner, R., Lass, A., and Puri, V. (2014) Fat-specific protein 27 (FSP27) interacts with adipose triglyceride lipase (ATGL) to regulate lipolysis and insulin sensitivity in human adipocytes. *J. Biol. Chem.* **289,** 12029–12039
21. Zhang, K., Shen, X., Wu, J., Sakaki, K., Saunders, T., Rutkowski, D. T., Back, S. H., and Kaufman, R. J. (2006) Endoplasmic reticulum stress activates cleavage of CREBH to induce a systemic inflammatory response. *Cell* **124,** 587–599
22. Zhang, C., Wang, G., Zheng, Z., Maddipati, K. R., Zhang, X., Dyson, G., Williams, P., Duncan, S. A., Kaufman, R. J., and Zhang, K. (2012) Endo-

plasmic reticulum-tethered transcription factor cAMP responsive element-binding protein, hepatocyte specific, regulates hepatic lipogenesis, fatty acid oxidation, and lipolysis upon metabolic stress in mice. *Hepatology* **55,** 1070–1082

23. Lee, M. W., Chanda, D., Yang, J., Oh, H., Kim, S. S., Yoon, Y. S., Hong, S., Park, K. G., Lee, I. K., Choi, C. S., Hanson, R. W., Choi, H. S., and Koo, S. H. (2010) Regulation of hepatic gluconeogenesis by an ER-bound transcription factor, *CREBH. Cell Metab.* **11,** 331–339
24. Lee, J. H., Giannikopoulos, P., Duncan, S. A., Wang, J., Johansen, C. T., Brown, J. D., Plutzky, J., Hegele, R. A., Glimcher, L. H., and Lee, A. H. (2011) The transcription factor cyclic AMP-responsive element-binding protein H regulates triglyceride metabolism. *Nat. Med.* **17,** 812–815